Available online at www.sciencedirect.com
ScienceDirect
Trans. Nonferrous Met. Soc. China 32(2022) 3238−3249
Transactions of Nonferrous Metals Society of China
www.tnmsc.cn

Effect of Ti−6Al−4V particle reinforcements on mechanical properties of Mg−9Al−1Zn alloy

Huan LUO[1], Jian-bo LI[1], Jun-liu YE[1], Jun TAN[1], Muhammad RASHAD[2], Xian-hua CHEN[1], Sheng-li HAN[3], Kai-hong ZHENG[3], Tian-tian ZHAO[4], Fu-sheng PAN[1]

1. College of Materials Science and Engineering, Chongqing University, Chongqing 400044, China;
2. Department of Chemical Sciences, Bernal Institute, University of Limerick, Limerick V94T9PX, Ireland;
3. Institute of New Materials, Guangdong Academy of Sciences, Guangzhou 510650, China;
4. Chongqing Institute of Quality & Standardization, Chongqing 400023, China

Received 19 August 2021; accepted 14 March 2022

Abstract: Mg−9Al−1Zn (AZ91) magnesium matrix composites reinforced by Ti−6Al−4V (TC4) particles were successfully prepared via powder metallurgical method. The yield strength (YS), ultimate tensile strength (UTS), and elongation (EL) showed a mountain-like tendency with the increase of the TC4 content. The mechanical properties of AZ91 magnesium matrix composites reached the optimal point with TC4 content of 10 wt.%, realizing YS, UTS, and EL of 335 MPa, 370 MPa, and 6.4%, respectively. The improvement of mechanical properties can be attributed to the effective load transfer from the magnesium matrix to the TC4 particles, dislocations associated with the difference in the coefficient of thermal expansion, good interfacial bonding between the Mg matrix and TC4 particles, and grain refinement strengthening.

Key words: magnesium matrix composites; powder metallurgy; mechanical properties; strengthening mechanisms

1 Introduction

Magnesium (Mg) is an ultralightweight structural metal, with a density of 1.74 g/cm^3, which is as light as two-thirds of aluminum (Al) [1]. Mg alloy and its composites exhibit various functionalities, including excellent heat-resistant [2], castability [3,4], damping performance, wear resistance [5,6], specific strength [7,8], and specific stiffness [9,10], thereby attracting considerable research attention for the critical structural applications [11−13]. To date, reinforcements realized by ceramic particles have been intensively investigated in Mg matrix composites [14−18]. Although the ceramic particle reinforcement strategy improved the mechanical strength of Mg matrix composites, low plasticity significantly limited their potential applications [19,20]. By contrast, metallic alternatives, such as Cu, Ni, Fe, and TC4 particles, possess high strength, ductility and elastic modulus [21]. Recent studies showed that the composites' strength and ductility can be improved by using titanium (Ti) and its alloy particles to reinforce Mg matrix composites rather than ceramic particles [22−25]. TC4 particles have the advantages of low density, high specific strength and hardness, high-temperature resistance, and good corrosion resistance. Previous studies confirmed that the ductility of TC4/AZ91 composites is better than that of SiC/AZ91 composites [26,27].

For sample preparation, secondary processing, such as hot extrusion, is used to refine the structure and improve the performance of magnesium matrix

Corresponding author: Jian-bo LI, Tel: +86-15723410753, E-mail: lijianbo1202@cqu.edu.cn; Jun TAN, E-mail: j.tan@cqu.edu.cn
DOI: 10.1016/S1003-6326(22)66016-3

composites. In the extrusion process, a fine and uniform recrystallized structure is introduced [28]. DENG et al [29] found that a uniform and dense composite can be obtained through secondary processing. ROY et al [30] reported that hot extrusion processing refines the matrix grains of the composite effectively. The dynamic recrystallization (DRX) of the matrix can be stimulated via the ceramic particle reinforcement, thereby making the grain size of Mg matrix finer. These examples are different to the extruded SiC/AZ91 composites, in which the damage of the reinforcement layer caused by the extrusion leads to the cracking of the particles [31]. However, specific research on Mg matrix composites reinforced by TC4 particles through the secondary processing technology is still limited.

In this work, TC4 particles with higher strength and plasticity than that of Mg alloy are chosen as reinforcement to improve the comprehensive properties of Mg matrix composites. The evolution of the microstructure and mechanical properties of TC4-reinforced Mg matrix composites prepared via powder metallurgy followed by hot extrusion were investigated. The effects of TC4 particles on the microstructure and mechanical properties of the Mg matrix composites were discussed.

2 Experimental

2.1 Raw materials

Mg powders (99.9% purity, 50−120 μm), Al powders (99.8% purity, 15−53 μm), zinc (Zn) powders (99.8% purity, 15−53 μm), and TC4 powders (99.8% purity, 15−53 μm) were used as raw materials to prepare AZ91 magnesium matrix composites. Figure 1 displays the SEM micrographs of the as-received Mg powders, Al powders, Zn powders, and TC4 powders. The morphologies of these powders are in irregular shape (Mg), and spherical shape (Al, Zn, TC4), respectively.

2.2 Preparation of composites

Mg matrix composites were prepared by using powder metallurgy method, including blending matrix element powders and reinforcing particles by mechanical stirring with ethanol as the medium. The mixed powders were then filtered, followed by vacuum drying, composite powder compaction, vacuum sintering to strengthen the powder compact, and hot extrusion, as shown in Fig. 2. This method does not need ball milling and is advantageous to avoiding heat generation during the preparation of the composites.

First, TC4 particles were mixed with ethanol

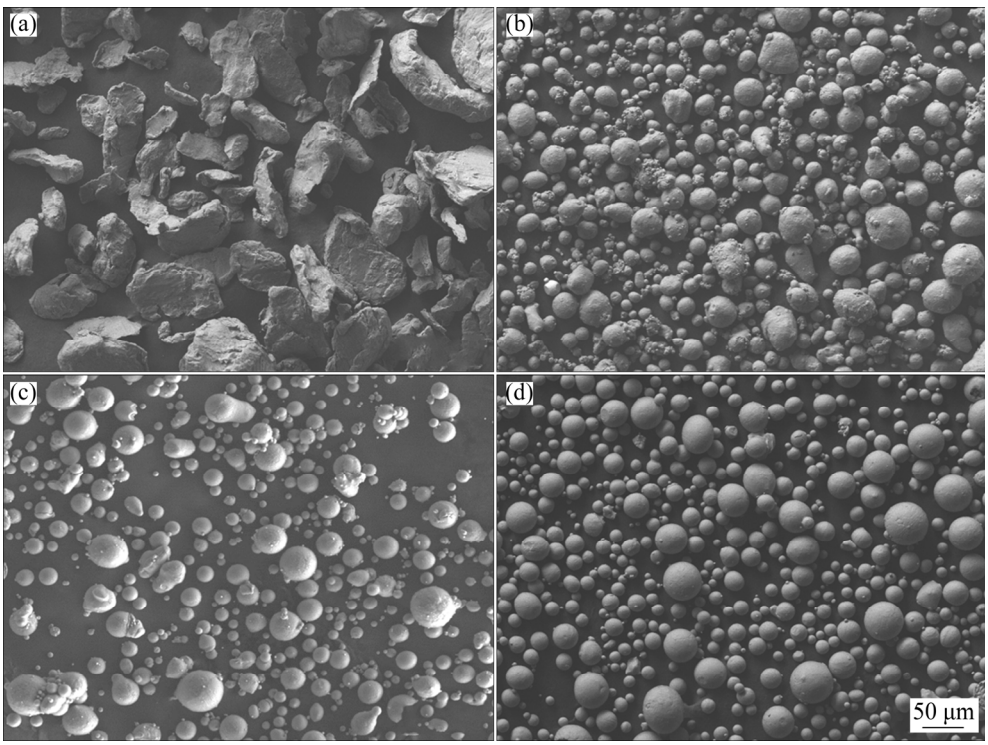

Fig. 1 SEM images of raw materials: (a) Mg powder; (b) Al powder; (c) Zn powder; (d) TC4 powder

for 30 min, and Mg, 9 wt.% Al and 1 wt.% Zn powders were mixed with ethanol and mechanically stirred at a rate of 1500 r/min. Second, the TC4 particle reinforcement dispersoid was introduced in the mixture of Mg, 9 wt.% Al and 1 wt.% Zn powders, and the stirring rate was kept at 2000 r/min. The mixing process was kept for 1.5 h to ensure the homogeneity of TC4 particles in matrix slurry. Finally, the composite slurry (TC4/Mg−9Al−1Zn) was filtered and dried in a vacuum oven at 60 °C for 15 h to synthesize the composite powders.

The mixed powders were pressed by using a hydraulic press with a pressure of 585 MPa to obtain pelletized samples with a diameter of 80 mm and a height of 35 mm. The pelletized samples were then sintered at 630 °C for 2.5 h in a tube furnace under a purified argon atmosphere. The samples were annealed at 350 °C for 1 h and then hot-extruded at an extrusion ratio of 25:1 to obtain a rod with a diameter of 16 mm, as shown in Fig. 3. The extrusion rate was set to 1 m/min.

2.3 Characterization and mechanical properties tests of materials

Phase identification was conducted through X-ray diffraction (XRD, D/MAX−1200, China) with Cu K_α radiation. The microstructures of the extruded samples were studied through optical microscopy, SEM (JEOL 7800F), energy dispersive

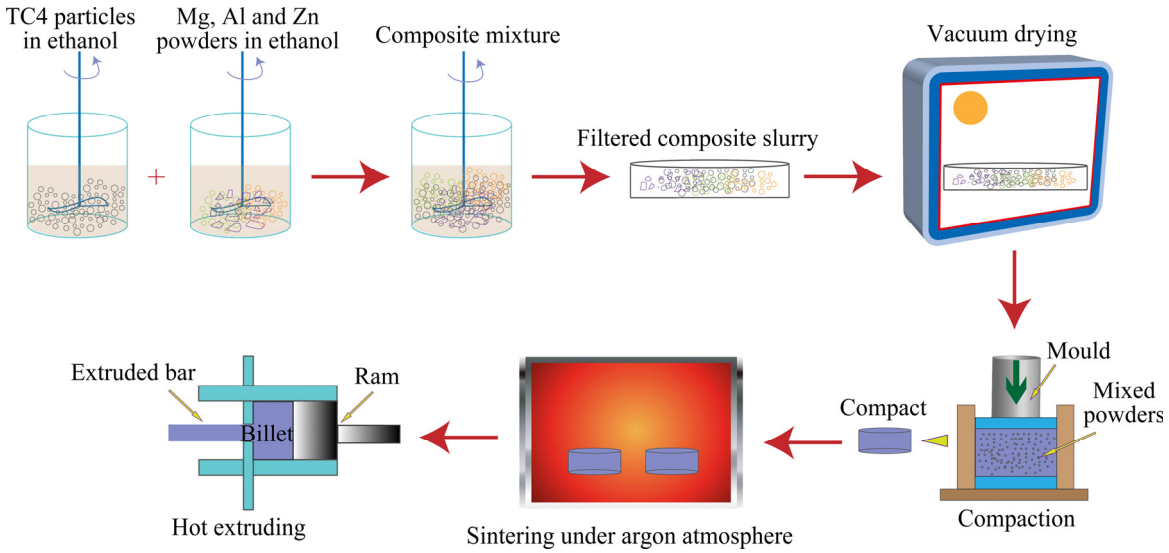

Fig. 2 Process flowchart of AZ91 composite fabrication using powder metallurgy method

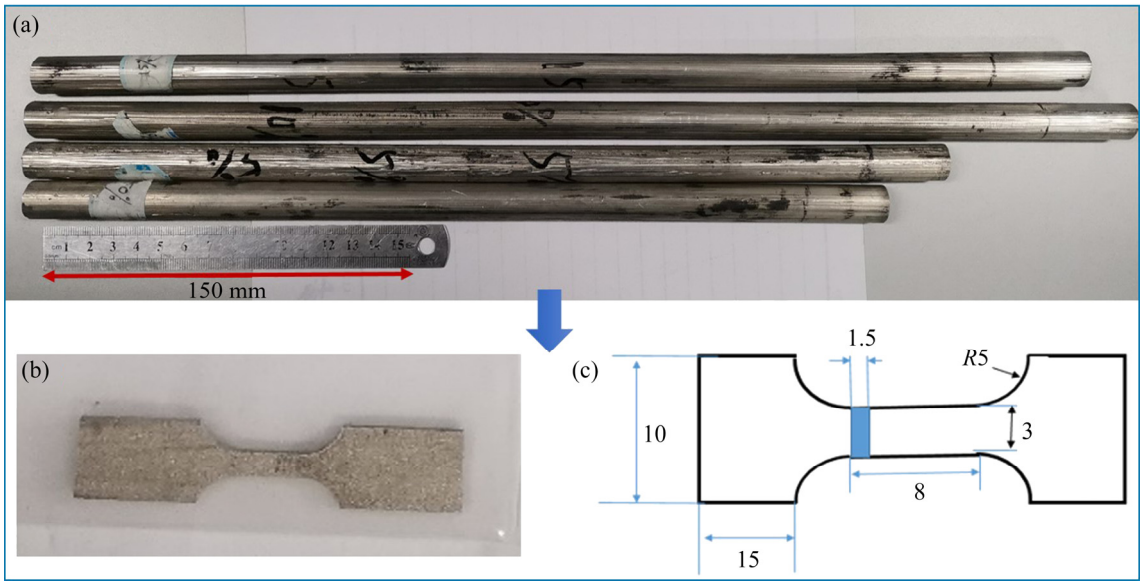

Fig. 3 Extruded bar (a), tensile sample (b), specific shape and size of specimen for tensile testing (c) of TC4/AZ91 composite (unit: mm)

spectroscopy (EDS), and backscattered electron (BSE) detection. The microhardness of AZ91−xTC4 (x=0, 5, 10, and 15 wt.%) composites was measured by using a microhardness tester (SHANGHAI HX−1000TM) under a load of 1 N and a dwell time of 10 s. For each sample, four sheet-shaped tensile samples with a gauge length of 8 mm, a width of 3 mm, and a thickness of 1.5 mm were cut from the extruded rods (Fig. 3), and the tensile rate was 0.5 mm/min.

3 Results

3.1 Density measurement

The theoretical density (ρ_t) of composites is determined by

$$\rho_t=\rho_m V_m+\rho_r V_r \quad (1)$$

where ρ_m, ρ_r, V_m and V_r are the densities of the matrix and reinforcement, and volume fractions of the matrix and reinforcement, respectively.

The relative density (ρ_r) of composites can be calculated by using the theoretical density (ρ_t) and the experimental density (ρ_e) as follows:

$$\rho_r=\frac{\rho_e}{\rho_t}\times 100\% \quad (2)$$

The relative density of composites as a function of TC4 content is shown in Fig. 4, and the results of relative density measurements are summarized in Table 1. The relative density of AZ91 alloy is lower than that of the composites, which is 96.44%. With the addition of TC4, its relative density monotonically increases and reaches more than 97%. The relative density of composites depends on many important factors, such as powder morphology, particle size, sintering process, and the dispersion of reinforcement particles in the matrix. In the experiment, the relative density of AZ91−TC4 composites is higher than that of AZ91 alloy.

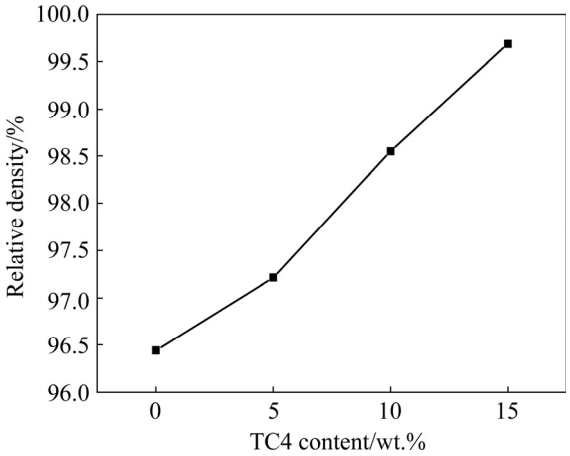

Fig. 4 Relative density of composites with different TC4 contents

3.2 Microstructure characterization

The XRD patterns of AZ91−xTC4 composites are depicted in Fig. 5. The peaks of all the as-extruded samples are derived from the Mg substrate and $Mg_{17}Al_{12}$ phases. Any peaks associated with zinc and aluminum are not observed because of their low mass fraction of constituents. The addition of TC4 particles causes new peaks associated with the α-Ti phase.

The grain characterization (size and morphology) of composites is exhibited in Fig. 6. The AZ91 alloy shows the maximal grain with a size of 29 μm, and the addition of micron-scale TC4 particles can effectively reduce the grain size of AZ91 matrix. The grains of the composites transform to smaller isometric grains after hot extrusion, suggesting that the DRX of matrix occurred during the extrusion process. In accordance with the previous report [32], the ceramic particles inhibited the flow of the matrix during the deformation process, resulting in local stress concentration around the grains. Such stress concentration causes high densities of dislocations and more orientation gradients around the grains.

Table 1 Density of composites with different TC4 contents

Material	TC4 content		Density/(g·cm^{-3})		Relative density/%
	w/%	φ/%	Theoretical	Experimental	
AZ91	0	0	1.8115	1.7470	96.44
AZ91−5TC4	5	2.11	1.8670	1.8150	97.21
AZ91−10TC4	10	4.35	1.9255	1.8976	98.55
AZ91−15TC4	15	6.73	1.9880	1.9818	99.69

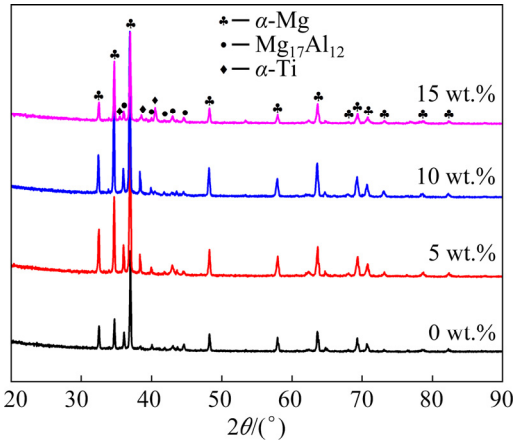

Fig. 5 XRD patterns of AZ91−*x*TC4 composites

Figure 7 shows the SEM images of composites. The Mg matrix possesses a smooth surface without microstructural defects, evidencing the improved adhesion between particles. The TC4 particles are homogeneously distributed in the Mg matrix. The $Mg_{17}Al_{12}$ precipitates exhibit a dispersive distribution for the 5 and 10 wt.% TC4. However, the $Mg_{17}Al_{12}$ precipitates present a blocky distribution when the content of TC4 increases to 15 wt.%. The interface between the TC4 and Mg matrix produces Al-rich phase products, as shown in Fig. 8. The precipitation of second phase is hindered because of the presence of TC4 reinforcements. The presence of Al-rich phase at the interface between reinforcement and Mg matrix may be derived from the diffusion from the matrix to the surrounding TC4 reinforcement particles. This process also leads to the Al-poor phase in the matrix, resulting in hindered precipitation of $Mg_{17}Al_{12}$. The presence of Al-rich phase also enhances the bonding between the reinforcement and Mg matrix.

Figure 9 exhibits the inverse pole figure (IPF) of AZ91−*x*TC4 composites. In accordance with the IPF figures, the grain size of the composites is refined from 7.53 to 5.71 μm with the addition of TC4 particles. The grain orientation of these samples is relatively random, showing no noticeable texture in the microstructure, and the microstructure is all-isotropic.

3.3 Mechanical properties

3.3.1 Vickers hardness

The Vickers hardness (HV) of AZ91−*x*TC4 composites is shown in Fig. 10. The microhardness is enhanced with the increasing content of TC4. When the content of TC4 particles reaches 15 wt.%, the AZ91 composite shows the largest hardness.

3.3.2 Tensile behavior

The tensile properties of composites are shown in Fig. 11. The yield strength (YS), ultimate tensile strength (UTS), and elongation (EL) of AZ91

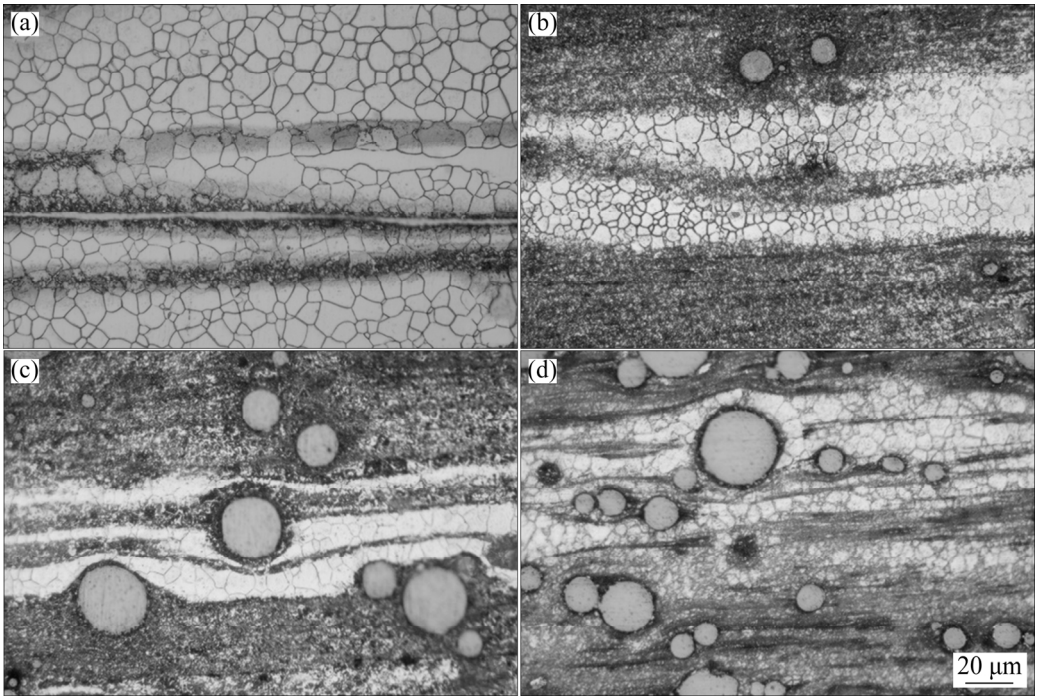

Fig. 6 Optical microscopy images showing particle characteristics of composites: (a) AZ91; (b) AZ91−5TC4; (c) AZ91−10TC4; (d) AZ91−15TC4

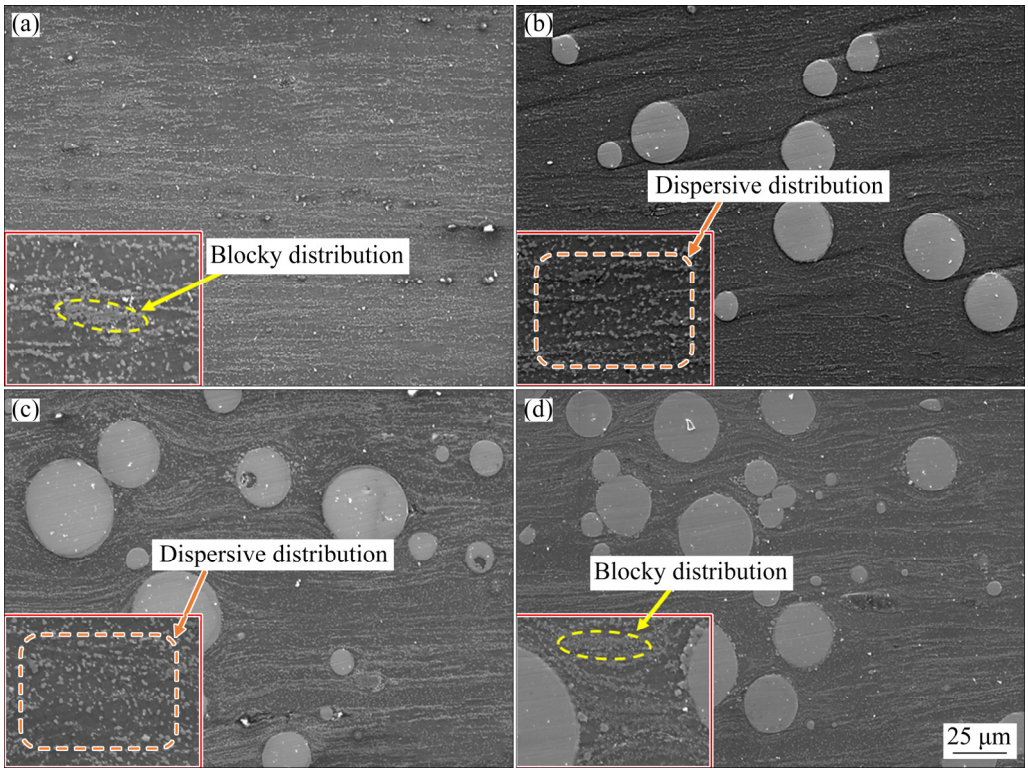

Fig. 7 SEM images showing surface morphology of composites: (a) AZ91; (b) AZ91−5TC4; (c) AZ91−10TC4; (d) AZ91−15TC4

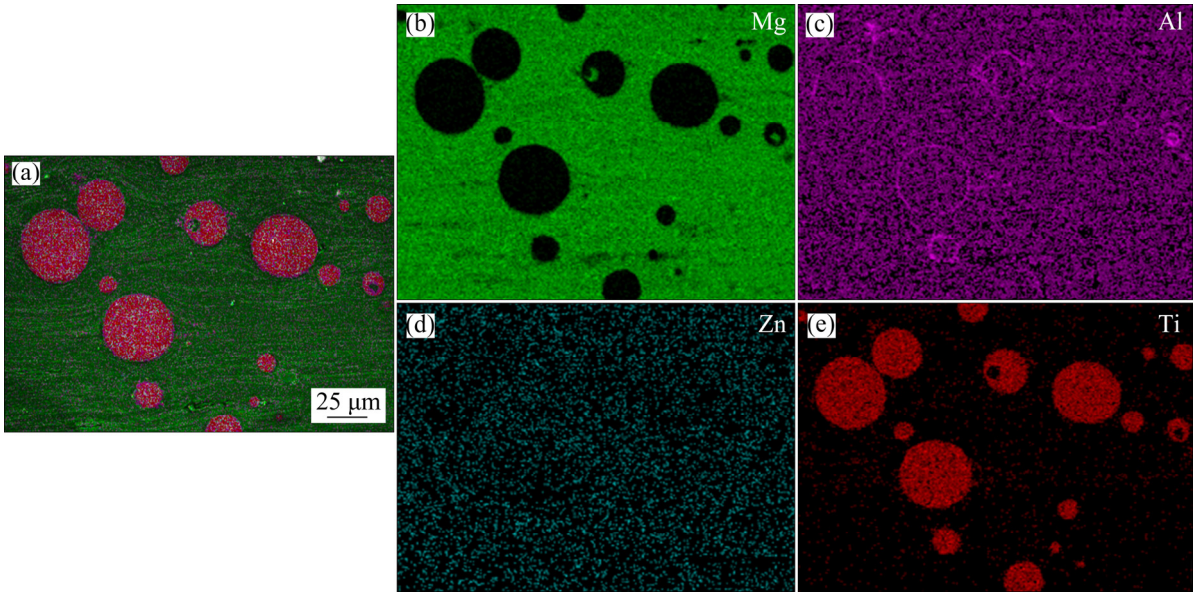

Fig. 8 SEM image (a) and corresponding EDS mapping results (b−e) of AZ91−10TC4 composite

composites increase with the increasing content of TC4 particles. When the content of TC4 reaches 10 wt.%, the composite obtains the optimal YS, UTS and EL, which are as large as 335 MPa, 370 MPa and 6.4%, respectively. The TC4 particles of the composites are uniformly dispersed in the matrix, leading to the strength improvement of the composites. However, the tensile strength and EL start to decrease when the content of TC4 particles exceeds 10 wt.%.

3.3.3 Work hardening capability

Work hardening denotes that the strength and hardness of metal materials increase, but the plasticity and toughness decrease with the increase

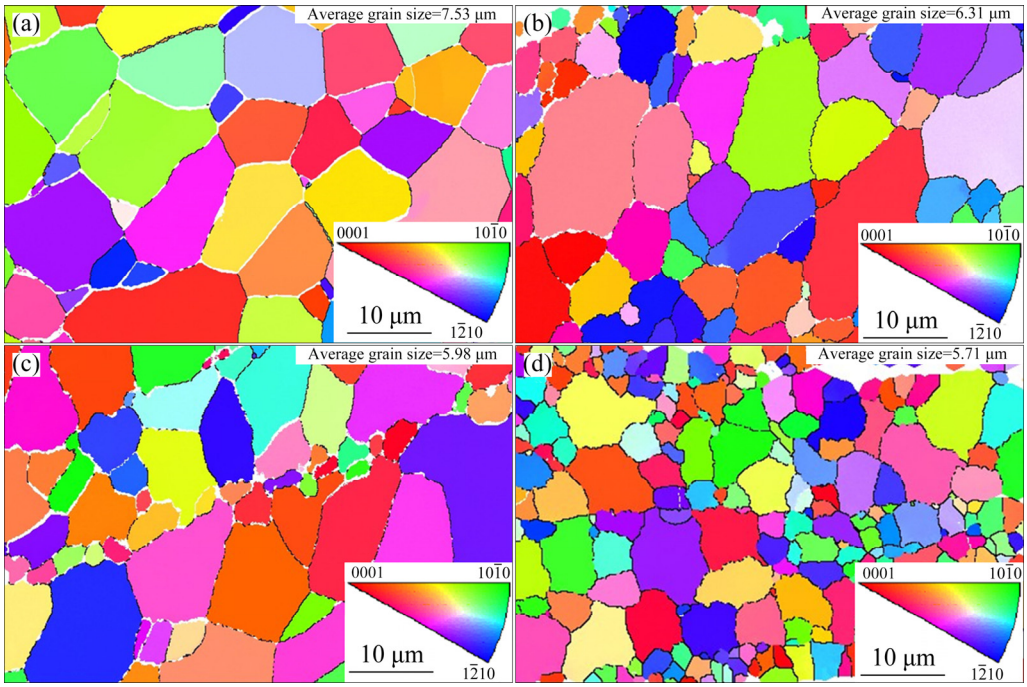

Fig. 9 IPF diagrams of composites: (a) AZ91; (b) AZ91−5TC4; (c) AZ91−10TC4; (d) AZ91− 15TC4

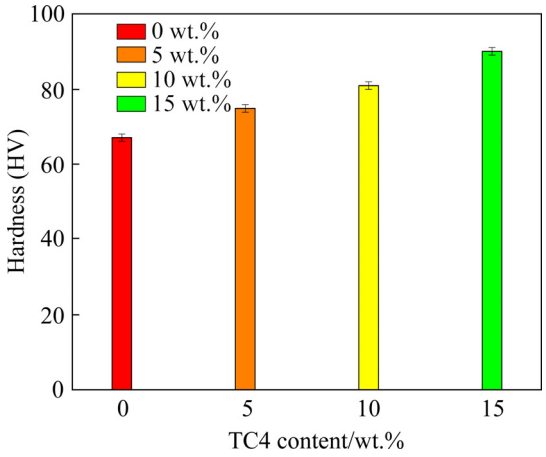

Fig. 10 Vickers hardness of AZ91 alloy and AZ91−*x*TC4 composites

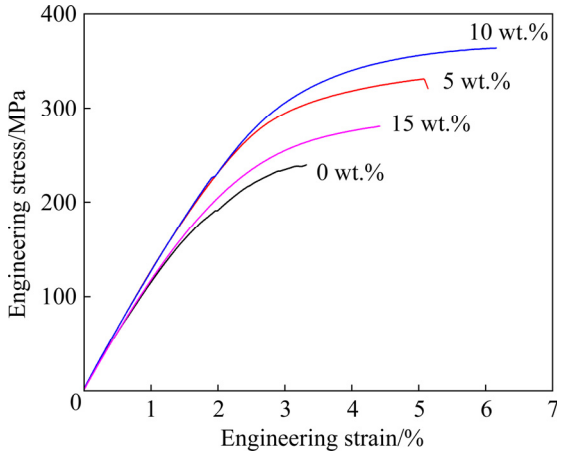

Fig. 11 Tensile properties of AZ91−*x*TC4 composites

in the degree of cold deformation [33]. The tensile true stress–strain curves of AZ91−*x*TC4 composites are obtained from the results in Fig. 11 to calculate the work hardening capacity, as shown in Fig. 12(a). With the increase in TC4 content, the true UTS of AZ91 composites increases significantly. The AZ91−10TC4 presents the highest true UTS of 386 MPa. Figure 12(b) displays the work hardening capacity of Mg matrix composites with different contents of TC4 particles. The work hardening capacity (H_c) is formulated as follows [34]:

$$H_c=\frac{\sigma_{true}^{UTS}-\sigma_{true}^{YS}}{\sigma_{true}^{YS}} \quad (3)$$

4 Discussion

4.1 Microhardness improvement

The enhanced hardness of composites can be ascribed to the following reasons. Relatively harder reinforcement (TC4) particles with uniform distribution are found. The Mg matrix is highly resistant to deformation when applying load due to the presence of reinforcement particles [35]. The diffusion of element at high sintering temperature makes the matrix and TC4 reinforcement host a good adhesion nature [36]. The unique structure of high specific surface area endows TC4 a large interfacial area with the Mg matrix.

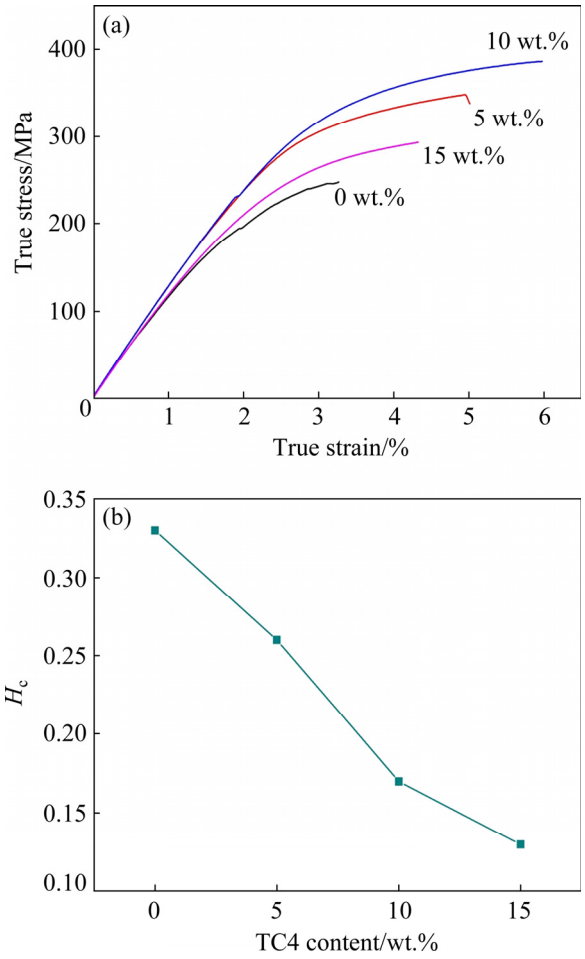

Fig. 12 Tensile true stress−strain (a) and work hardening capacity (b) of AZ91−*x*TC4 composites

4.2 Strengthening mechanism

The mechanical properties of the composites are obviously improved with the appropriate addition of TC4 particles. The strengthening mechanisms of particle-reinforced materials can be summarized as direct and indirect strengthening mechanisms [37].

The former is derived from the load transfer from the matrix to the reinforcement, which is mainly due to the interface bonding between the matrix, the intermetallic phase, and the reinforcement. In this work, the load can be effectively transferred from the Mg matrix to the TC4 particles with the stress, making a significant increase in strength of the composites. The improvement in YS of the composites contributes to load transfer mechanism, which is described as $\sigma_{L.T}=f\sigma_m/2$ [38], where σ_m is the YS of the matrix, and f is the proportion of the particles. When the TC4 content ranges from 5 wt.% to 15 wt.%, the corresponding increase in $\sigma_{L.T}$ is 5.75, 11.5, and 17.25 MPa, respectively. This finding confirms the direct strengthening mechanism through load transfer, and the strengthening effect is better with larger $\sigma_{L.T}$.

The latter is that the addition of reinforcement particles changes the microstructure and deformation mode of the composites, such as dislocation strengthening [39].The TC4 particles and $Mg_{17}Al_{12}$ intermetallic compound can impede the movement of dislocations in the matrix with the application of load. The coherence relationship between the precipitates and the matrix directly affects the mode of action between the precipitates and dislocations [40]. During the synthesis of the composites, the matrix and the reinforcing phase may produce grand residual stress or strain heap due to the diversity in the coefficient of thermal expansion (CTE) between the matrix (2.6×10^{-5} K^{-1}) and the reinforcements (9.4×10^{-6} K^{-1}). The improvement in YS of the composites is the result of distinction in CTE, which is imparted by $\sigma_{CTE}=0.2MGb\sqrt{\rho}$ [41], where M is the average orientation factor of Mg (M=6.5), the constant 0.2 characterizes the transparency of the dislocation forest of the substrate–substrate dislocation interaction in Mg at room temperature, G is the shear modulus (16.6 GPa), b is the magnitude of the Burgers vector (0.321 nm), and ρ is the dislocation density imparted by $\rho=\dfrac{12\sqrt{2}\Delta\alpha\Delta Tf}{bd(1-f)}$, where $\Delta\alpha$ is the difference in CTE (1.7×10^{-5} K^{-1}), ΔT is the temperature change (325 °C), and d is the mean size of the spherical particles (approximately 29 μm). The dislocation density in composites with TC4 content of 5−15 wt.% can be determined as 9.75×10^{11}, 2.01×10^{12} and 3.27×10^{12} m^{-2}. When the TC4 content ranges from 5 to 15 wt.%, the σ_{CTE} of YS increases to 5.04, 7.33 and 9.24 MPa, suggesting the presence of indirect strengthening mechanism through the different CTEs, and the strengthening effect is better with larger σ_{CTE}.

The tensile EL of composites reduces when the TC4 content increases from 10 to 15 wt.%, which might be due to the agglomeration of TC4 reinforcement particles. This results in crack initiation at the interfacial zone, thereby reducing the ductility of the composite. Although friable

$Mg_{17}Al_{12}$ particles with blocky distribution can cause brittleness of the grain boundary and crack initiation inside the matrix, the precipitation of $Mg_{17}Al_{12}$ intermetallic compounds presents dispersive distribution when TC4 reinforcement particles are appropriately introduced in the composites, thereby reducing their stress concentration. Simultaneously, the load can be effectively transferred from the magnesium matrix to the TC4 particles. Thus, the tensile strength and ductility of the composites are improved.

The strength and plasticity of the obtained composites are higher than those reported in previous studies [26,27,42], as listed in Table 2. The AZ91−TC4 composites are prepared through different smelting processes [26,27]. The average grain size decreases with the increasing content of particles. The TC4 particles bond well with the matrix. Some interfacial reactions are observed in the composites. However, the composites are fabricated by smelting, which causes the inhomogeneous distribution of TC4 particles in the matrix due to the sedimentation during the smelting process. The tensile strength and plasticity of the composites are restricted with the UTS and EL of 245 MPa and 3.9%, respectively. In this study, the AZ91−TC4 composites are prepared by powder metallurgy method, and the TC4 reinforcement particles distribute in the magnesium matrix uniformly. Some studies were reported on AZ91−SiC composites using SiC ceramic particle as reinforcement [42,43]. The UTS and EL of the composites are 152 MPa and 0.8%, respectively.

Table 2 Comparison of mechanical properties of AZ91−TC4 composites with previous studies

Material	YS/ MPa	UTS/ MPa	EL/ %
AZ91 (this work)	230	240	3.3
AZ91−5wt.%TC4 (this work)	302	321	5.2
AZ91−10wt.%TC4 (this work)	335	370	6.4
AZ91−15wt.%TC4 (this work)	263	280	4.4
As-cast AZ91−10vol.%TC4 [27]	125	245	3.9
As-extruded AZ91−10vol.%TC4 [27]	249	369	6.4
Cast AZ91−20vol.%TC4 [26]	−	154	0.5
AZ91−10vol.%SiC [42]	135	152	0.8

The low ductility is due to the appearance of localized damages, such as interface debonding in the fracture process of the composites. The Mg matrix composites reinforced by ceramic particles show high strength but low plasticity, which limits their potential applications. Metallic particles possess improved strength, ductility, and elastic modulus [37]. The experimental results show that the strength and ductility of the prepared AZ91−TC4 composites are higher than those of the Mg matrix composites reinforced by ceramic particles with high volume fraction.

4.3 Work hardening mechanism

The variation of work hardening capacity is closely related to the dislocation movements in as-extruded material [44]. When dislocations are piled up around the periphery of TC4 particles, the particles activate a sliding system to transfer stress, efficiently reducing stress concentration [45]. The decreased stress concentration reduces the work hardening capacity to a certain extent. Thus, the work hardening capacity decreases with the increase in TC4 content, and the plasticity of the composites is improved.

4.4 Fracture mechanism

The tensile fracture morphology of AZ91−*x*TC4 composites is displayed in Fig. 13. The tensile fracture surface morphology shows that the fracture mechanism of composites is ductile fracture (Figs. 13(a−d)). The SEM images of the fracture of the composites show dimples and tear ridges, as displayed in Figs. 13(b, c, d), indicating the ductility of the composites, which agrees well with the EL of the composites. In other studies, the fractured surface of SiC/AZ91 composites shows that the cracks are close to the ceramic particles, causing the fracture of the composites and the debonding of particles from the matrix [29,46]. In the present work, the TC4 particles are discovered within the dimples, as displayed in Figs. 13(f, g, h). The interfacial debonding and microcracks rarely appear regardless of a few small dimples in the fracture of the composites. This proves that the TC4 particles can improve the interface bonding between the reinforcement particles and the matrix, further enhancing the mechanical properties of the composites.

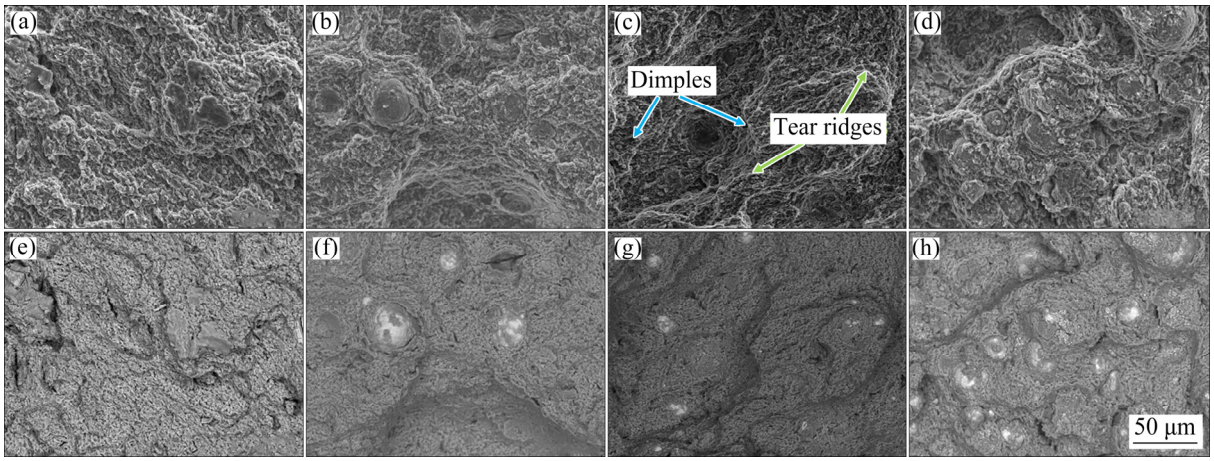

Fig. 13 SEM (a−d) and BSE (e−h) images of fractured surface of AZ91−*x*TC4 composites (a, e) *x*=0 wt.%; (b, f) *x*=5 wt.%; (c, g) *x*=10 wt.%; (d, h) *x*=15 wt.%

5 Conclusions

(1) AZ91 magnesium matrix composites reinforced by TC4 particles exhibited a great improvement in tensile strength compared with AZ91 alloy. The improvement of mechanical properties can be attributed to the effective load transferring from the magnesium matrix to the TC4 particles, dislocations produced by the difference in the CTE, good interfacial bonding between the Mg matrix and TC4 particles, and fine-grain strengthening.

(2) With the increase in the TC4 content, the tensile strength, elongation, and hardness increased simultaneously. However, when the TC4 content exceeded 10 wt.%, the strength and elongation began to reduce.

Acknowledgments

The authors acknowledge the financial support from the Guangdong Major Project of Basic and Applied Basic Research, China (No. 2020B0301030006), the National Natural Science Foundation of China (Nos. 52171133, 52171103), the "111 Project" by the Ministry of Education of China (No. B16007), and Fundamental Research Fund of Central Universities in China (No. 2018CDJDCL0019). The author would like to thank Joint Lab for electron microscopy of Chongqing University.

References

[1] PRASAD S V S, PRASAD S B, VERMA K, MISHRA R K, KUMAR V, SINGH S. The role and significance of Magnesium in modern day research-A review [J]. Journal of Magnesium and Alloys, 2021, DOI: doi.org/10.1016/j.jma.2021.05.012.

[2] ZHANG Su-qing, CHEN Ti-jun, ZHOU Ji-xue. Effects of punch velocity on microstructure and tensile properties of thixoforged Mg_2Si_p/AM60B composite [J]. Transactions of Nonferrous Metals Society of China, 2020, 30(1): 110−122.

[3] RASHAD M, PAN Fu-sheng, GUO Wei, LIN Han, ASIF M, IRFANE M. Effect of alumina and silicon carbide hybrid reinforcements on tensile, compressive and micro-hardness behavior of Mg−3Al−1Zn alloy [J]. Materials Characterization, 2015, 106: 382−389.

[4] NIE Kai-bo, ZHU Zhi-hao, MUNROE P, DENG Kun-kun, GUO Ya-chao. Microstructure and mechanical properties of TiC nanoparticle-reinforced Mg−Zn−Ca matrix nano-composites processed by combining multidirectional forging and extrusion [J]. Transactions of Nonferrous Metals Society of China, 2020, 30(9): 2394−2412.

[5] AL-MAAMARI A E A, IQBAL A A, NURUZZAMAN D M. Wear and mechanical characterization of Mg−Gr self-lubricating composite fabricated by mechanical alloying [J]. Journal of Magnesium and Alloys, 2019, 7: 283−290.

[6] RAHMANI K, MAJZOOBI G H, EBRAHIM-ZADEH G, KASHFI M. Comprehensive study on quasi-static and dynamic mechanical properties and wear behavior of Mg−B_4C composite compacted at several loading rates through powder metallurgy [J]. Transactions of Nonferrous Metals Society of China, 2021, 31(2): 371−381.

[7] ZHOU Xia, LIU Zi-fan, SU Feng, FAN Ya-fu. Magnesium composites with hybrid nano-reinforcements: 3D simulation of dynamic tensile response at elevated temperatures [J]. Transactions of Nonferrous Metals Society of China, 2021, 31(3): 636−647.

[8] XU Tian-cai, YANG Yan, PENG Xiao-dong, SONG Jiang-feng, PAN Fu-sheng. Overview of advancement and development trend on magnesium alloy [J]. Journal of Magnesium and Alloys, 2019, 7: 536−544.

[9] ZHAO Jian-hua, ZHAO Wen-qun, QU Shen, ZHANG Yan-qing. Microstructures and mechanical properties of AZ91D/0Cr19Ni9 bimetal composite prepared by liquid−

solid compound casting [J]. Transactions of Nonferrous Metals Society of China, 2019, 29(1): 51−58.

[10] MOHAMA D, RODZI S N H, ZUHAILAWATI H, DHINDAW B K. Mechanical and degradation behaviour of biodegradable magnesium–zinc/hydroxyapatite composite with different powder mixing techniques [J]. Journal of Magnesium and Alloys, 2019, 7: 566−576.

[11] YANG Yan, XIONG Xiao-ming, CHEN Jing, PENG Xiao-dong, CHEN Dao-lun, PAN Fu-sheng. Research advances in magnesium and magnesium alloys worldwide in 2020 [J]. Journal of Magnesium and Alloys, 2021, 9: 705−747.

[12] WU Liang, DING Xing-xing, ZHENG Zhi-cheng, TANG Ai-tao, ZHANG Gen, ATRENS A, PAN Fu-sheng. Doublely-doped Mg−Al−Ce−$V_2O_7^{4-}$ LDH composite film on magnesium alloy AZ31 for anticorrosion [J]. Journal of Materials Science & Technology, 2021, 64: 66−72.

[13] GUO Su-qing, WANG Ri-chu, PENG Chao-quan, CAI Zhi-yong, DONG Cui-ge. Microstructures and mechanical properties of Ni-coated SiC particles reinforced AZ61 alloy composites [J]. Transactions of Nonferrous Metals Society of China, 2019, 29(9): 1854−1863.

[14] RAHMANI K, SADOOGHI A, HASHEMI S J. The effect of Al_2O_3 content on tribology and corrosion properties of Mg−Al_2O_3 nanocomposites produced by single and double-action press [J]. Materials Chemistry and Physics, 2020, 250: 123058.

[15] SHEN M J, WANG X J, ZHANG M F, HU X S, ZHENG M Y, WU K. Fabrication of bimodal size SiC_p reinforced AZ31B magnesium matrix composites [J]. Materials Science and Engineering A, 2014, 601: 58−64.

[16] FERKEL H, MORDIKE B L. Magnesium strengthened by SiC nanoparticles [J]. Materials Science and Engineering A, 2001, 298: 193−199.

[17] RAHMANI K, NOURI A, WHEATLEY G, MALEKMOHAMMADI H, BAKHTIARI H, YAZDI V. Determination of tensile behavior of hot-pressed Mg−TiO_2 and Mg−ZrO_2 nanocomposites using indentation test and a holistic inverse modeling technique [J]. Journal of Materials Research and Technology, 2021, 14: 2107−2114.

[18] RAHMANI K, MAJZOOBI G H, BAKHTIARI H, SADOOGHI A. On the effect of compaction velocity, size, and content of reinforcing particles on corrosion resistance of Mg−B_4C composites [J]. Materials Chemistry and Physics, 2021, 271: 124946.

[19] ZHANG Xue-zhi, ZHANG Qiang, HU H. Tensile behaviour and microstructure of magnesium AM60-based hybrid composite containing Al_2O_3 fibres and particles [J]. Materials Science and Engineering A, 2014, 607: 269−276.

[20] SHEN M J, WANG X J, LI C D, ZHANG M F, HU X S, ZHENG M Y, WU K. Effect of submicron size SiC particles on microstructure and mechanical properties of AZ31B magnesium matrix composites [J]. Materials & Design, 2014, 54: 436−442.

[21] DINAHARAN I, ZHANG Shuai, CHEN Gao-qiang, SHI Qing-yu. Assessment of Ti−6Al−4V particles as a reinforcement for AZ31 magnesium alloy-based composites to boost ductility incorporated through friction stir processing [J]. Journal of Magnesium and Alloys, 2022, 10(4): 979−992.

[22] ZHANG Chun-lei, WANG Xiao-jun, WANG Xiao-ming, HU Xiao-shi, WU Kun. Fabrication, microstructure and mechanical properties of Mg matrix composites reinforced by high volume fraction of sphere TC4 particles [J]. Journal of Magnesium and Alloys, 2016, 4: 286−294.

[23] SANKARANARAYANAN S, JAYALAKSHMI S, GUPTA M. Hybridizing micro-Ti with nano-B_4C particulates to improve the microstructural and mechanical characteristics of Mg−Ti composite [J]. Journal of Magnesium and Alloys, 2014, 2: 13−19.

[24] RASHAD M, PAN F S, ASIF M, SHE Jia, ULLAH A. Improved mechanical proprieties of "magnesium based composites" with titanium-aluminum hybrids [J]. Journal of Magnesium and Alloys, 2015, 3: 1−9.

[25] ZHOU Hai-ping, HU Lian-xi, SUN Hong-fei, CHEN Xian-jue. Synthesis of nanocrystalline Mg-based Mg−Ti composite powders by mechanical milling [J]. Materials Characterization, 2015, 106: 44−51.

[26] WANG X M, WANG X J, HU X S, WU K, ZHENG M Y. Processing, Microstructure and mechanical properties of Ti6Al4V particles-reinforced Mg matrix composites [J]. Acta Metallurgica Sinica (English Letters), 2016, 29: 940−950.

[27] WANG Xiao-jun, WANG Xiao-ming, HU Xiao-shi, WU Kun. Effects of hot extrusion on microstructure and mechanical properties of Mg matrix composite reinforced with deformable TC4 particles [J]. Journal of Magnesium and Alloys, 2020, 8: 421−430.

[28] KHORASANI F, EMAMY M, MALEKAN M, MIRZADEH H, POURBAHARI B, KRAJNÁK T, MINÁRIK P. Enhancement of the microstructure and elevated temperature mechanical properties of as-cast Mg−Al_2Ca−Mg_2Ca in-situ composite by hot extrusion [J]. Materials Characterization, 2019, 147: 155−164.

[29] DENG K K, WU K, WU Y W, NIE K B, ZHENG M Y. Effect of submicron size SiC particulates on microstructure and mechanical properties of AZ91 magnesium matrix composites [J]. Journal of Alloys and Compounds, 2010, 504: 542−547.

[30] ROY S, KANNAN G, SUWAS S, SURAPPA M K. Effect of extrusion ratio on the microstructure, texture and mechanical properties of $(Mg/AZ91)_m$−SiC_p composite [J]. Materials Science and Engineering A, 2015, 624: 279−290.

[31] WANG X J, WU K, ZHANG H F, HUANG W X, CHANG H, GAN W M, ZHENG M Y, PENG D L. Effect of hot extrusion on the microstructure of a particulate reinforced magnesium matrix composite [J]. Materials Science and Engineering A, 2007, 465: 78−84.

[32] DOHERTY R D, HUGHES D A, HUMPHREYS F J, JONAS J J, JENSEN D J, KASSNER M E, KING W E, MCNELLEY T R, MCQUEEN H J, ROLLETT, A D. Current issues in recrystallization: A review [J]. Materials Science and Engineering A, 1997, 238: 219−274.

[33] WU Bo, LI Jian-bo, LIU Li-zi, CHEN Xian-hua, TAN Jun, SONG Jiang-feng, RASHAD M, PAN Fu-sheng. Effect of Zener–Hollomon parameter on high-temperature deformation behaviors of Mg−6Zn−1.5Y−0.5Ce−0.4Zr Alloy [J]. Acta Metallurgica Sinica (English Letters), 2021, 34: 606−616.

[34] AFRIN N, CHEN D L, CAO X, JAHAZI M. Strain hardening behavior of a friction stir welded magnesium alloy [J]. Scripta Materialia, 2007, 57: 1004−1007.
[35] LEE C, WEI Xiao-ding, KYSAR J W, HONE J. Measurement of the elastic properties and intrinsic strength of monolayer graphene [J]. Science, 2008, 321: 385−388.
[36] RASHAD M, PAN Fu-sheng, TANG Ai-tao, ASIF M, AAMIR M. Synergetic effect of graphene nanoplatelets (GNPs) and multi-walled carbon nanotube (MW-CNTs) on mechanical properties of pure magnesium [J]. Journal of Alloys and Compounds, 2014, 603: 111−118.
[37] YAN Y W, GENG L, LI A B. Experimental and numerical studies of the effect of particle size on the deformation behavior of the metal matrix composites [J]. Materials Science and Engineering A, 2007, 448: 315−325.
[38] AIKIN R M Jr, CHRISTODOULOU L. The role of equiaxed particles on the yield stress of composites [J]. Scripta Metallurgica et Materialia, 1991, 25: 9−14.
[39] DOBROŇ P, DROZDENKO D, FEKETE K, KNAPEK M, BOHLEN J, CHMELÍK F. The slip activity during the transition from elastic to plastic tensile deformation of the Mg−Al−Mn sheet [J]. Journal of Magnesium and Alloys, 2021, 9: 1057−1067.
[40] LI Jing-jing, JU Jiang, ZHANG Zhen, ZHOU Yang, LUO Yi-fei, MUDI Kun-qi, XIE Yue-huang, WANG Meng-meng, LIANG Jia-miao, WANG Jun. Precipitation behavior and mechanical properties of Al−Zn−Mg−Cu matrix nanocomposites: Effects of SiC nanoparticles addition and heat treatment [J]. Materials Characterization, 2021, 172: 110827.
[41] HAN B Q, DUNAND D C. Microstructure and mechanical properties of magnesium containing high volume fractions of yttria dispersoids [J]. Materials Science and Engineering A, 2000, 277: 297−304.
[42] LUO A. Processing, microstructure, and mechanical behavior of cast magnesium metal matrix composites [J]. Metallurgical and Materials Transactions A, 1995, 26: 2445−2455.
[43] CHUA B W, LU L, LAI M O. Influence of SiC particles on mechanical properties of Mg based composite [J]. Composite Structures, 1999, 47: 595−601.
[44] ZHAO Chao-yue, CHEN Xian-hua, PAN Fu-sheng, GAO Shang-yu, ZHAO Di, LIU Xiao-fang. Effect of Sn content on strain hardening behavior of as-extruded Mg−Sn alloys [J]. Materials Science and Engineering A, 2018, 713: 244−252.
[45] JOSEPH S, BANTOUNAS I, LINDLEY T C, DYE D. Slip transfer and deformation structures resulting from the low cycle fatigue of near-alpha titanium alloy Ti-6242Si [J]. International Journal of Plasticity, 2018, 100: 90−103.
[46] FATHI R, MA A, SALEH B, XU Qiong, JIANG Jing-hua. Investigation on mechanical properties and wear performance of functionally graded AZ91−SiC_p composites via centrifugal casting [J]. Materials Today Communications, 2020, 24: 101169.

Ti−6Al−4V 颗粒增强体对 Mg−9Al−1Zn 合金力学性能的影响

罗 欢[1]，李建波[1]，叶俊锣[1]，谭 军[1]，Muhammad RASHAD[2]，
陈先华[1]，韩胜利[3]，郑开宏[3]，赵甜甜[4]，潘复生[1]

1. 重庆大学 材料科学与工程学院，重庆 400044；
2. Department of Chemical Sciences, Bernal Institute, University of Limerick, Limerick V94T9PX, Ireland；
3. 广东省科学院 新材料研究所，广州 510650；
4. 重庆市质量与标准化研究院，重庆 400023

摘 要：采用粉末冶金法制备 Ti−6Al−4V(TC4)颗粒增强 Mg−9Al−1Zn(AZ91)镁基复合材料。随着 TC4 含量的增加，复合材料的屈服强度、极限抗拉强度和伸长率先升高后降低。当 TC4 颗粒的含量达到 10%(质量分数)时，复合材料具有优异的综合力学性能，其屈服强度、抗拉强度和伸长率分别为 335 MPa、370 MPa 和 6.4%。综合力学性能的改善是由于镁基体和 TC4 颗粒之间具有良好的界面结合，载荷可从镁基体转移到 TC4 颗粒上，其强化机制主要包括热膨胀系数差异引起的位错强化及细晶强化。

关键词：镁基复合材料；粉末冶金；力学性能；强化机制

(Edited by Xiang-qun LI)